Carbohydrate Polymers 114 (2014) 65–72

Contents lists available at ScienceDirect

Carbohydrate Polymers

journal homepage: www.elsevier.com/locate/carbpol

Adsorption and photocatalytic degradation of 2-CP in wastewater onto CS/$CoFe_2O_4$ nanocomposite synthesized using gamma radiation

Manal F. Abou Taleb[a,b,*]

[a] Chemistry Department College of Science and Humanities, Salman bin Abdulaziz University, Alkharj, Saudi Arabia
[b] Polymer Chemistry Department, National Center for Radiation Research and Technology, PO Box No. 29, Nasr city, Cairo 11731, Egypt

ARTICLE INFO

Article history:
Received 7 May 2014
Received in revised form 10 July 2014
Accepted 29 July 2014
Available online 7 August 2014

Keywords:
$CoFe_2O_4$
Photocatalysis
2-Chlorophenol
Degradation
Gamma radiation

ABSTRACT

Photocatalytic degradation of 2-chlorophenol (2-CP) was studied using the photocatalyst chitosane/$CoFe_2O_4$ nanocomposite (CS/CF) under visible light. CS/CF nanocomposites were synthesized via gamma irradiation cross-linking method with the aid of sonication. Physical characteristics of CS/CF were studied using infrared spectrophotometer (IR), scanning electron microscopy (SEM), transmission electron microscope (TEM) and ultraviolet–visible (UV–vis) spectroscopy. Their photocatalytic activity was tested for the degradation of 2-CP in aqueous medium using sunlight. The effect of different parameters such as catalyst concentration, 2-CP concentration and reaction pH on degradation was also examined. It was verified that the 2-CP degradation rate fits a pseudo-first-order kinetics for initial 2-CP concentrations between 25 and 100 mg/l, at 30 °C. The degradation kinetics fit well Langmuir–Hinshelwood rate law. The degradation of (2-CP) follows pseudo-first-order kinetics. Results showed that after the catalyst had been used 5 times repeatedly, the degradation rate was still above 80%.

1. Introduction

The photocatalytic oxidation is one of the emerging technologies for the elimination of organic micropollutants because of the efficiency in their mineralization, ideally producing as end products carbon dioxide, water, and inorganic mineral ions (Qourza, Barka, Tamimi, Assabbane, & Ait-Ichou, 2008; Sobczyński, Duczmal, & Zmudziński, 2004; Bahnemann, 2004; Hu & Yuan, 2005; Sivalingam & Madras, 2004). Photocatalysis has been an active area of research for several years owing to its potential application in water decontamination and hydrogen production (Palanisamy, Babu, Sundaravel, Anandan, & Murugesan, 2013). The interest in magnetic nanoparticles (MNPs) and nanocomposites (MNCs) has greatly increased in recent years not only because of their broad applications in several technological fields including ferrofluids, magnetic data storage, magneto optical, magnetic resonance imaging, medicine, and drug delivery systems, but also due to their relevance from the point of fundamental physics (Shafi, Gedanken, Prozorov, & Balogh, 1998; Zhu et al., 2010). MNPs are also used extensively for catalytic purposes (Casbeer, Sharma, & Li, 2012). Photocatalysts utilize photon energy to carry out oxidation and reduction reactions. When irradiated with light energy, an electron (e^-) is excited from the valence band (VB) to the conduction band (CB) of the photocatalyst, leaving a photogenerated hole (h^+). This creates hydroxyl ions in aqueous solution thus facilitating catalytic activities (Casbeer et al., 2012; Zhang, Chen, & Bahnemann, 2009a). For a material to qualify as a good photocatalyst needs a relatively large band gap, larger surface area, and nonagglomeration of particles. Cubic $CoFe_2O_4$ has been widely studied due to its high electromagnetic performance, excellent chemical stability, mechanical hardness and high cubic magnetocrystalline anisotropy (Zi et al., 2009).

2-Chlorophenol (2-CP) was chosen as model target pollutant because it is widely used in industry and daily life, and have caused considerable damage and threat to the aquatic ecosystem and human health (Ananpattarachai, Kajitvichyanukul, & Seraphin, 2009; Gryglik, Miller, & Ledakowicz, 2007). 2-CP is potentially a carcinogenic and mutagenic to mammalian as well as aquatic life. It is listed among the priority water pollutant by US EPA (Janda & Svecova, 2000). It is generated as a by-product in plastic, paper making, insecticidal and petrochemical industries. It can cause serious effects on human health and environment (Yue et al., 2002). Hence, design of a suitable process for complete mineralization of 2-chlorophenol in aqueous medium is an important issue. Photodegradation process of 2-chlorophenol pollutants has attracted

* Corresponding author at: National Center for Radiation Research and Technology, Department of Polymer Chemistry, PO Box No. 29, Naser 11731, Egypt. Tel.: +20 1221423531/+966541314733; fax: +20 22274929.
E-mail addresses: abutalib_m@yahoo.com, m.aboutaleb@sau.edu.sa, manotalib222@yahoo.de

http://dx.doi.org/10.1016/j.carbpol.2014.07.061
0144-8617/

increasing attention during the past decades (Ananpattarachai et al., 2009; Ku, Li, Wang, Ma, & Chou, 2010; Song & Kang, 2008; Mogyor´si, Farkas, Dékny, Ilisz, & Dombi, 2002; Barakat, Schaeffer, Hayes, & Ismat-Shah, 2004). The photocatalytic degradation of 4-chlorophenol was extensively studied under UV-light illumination using MgAl hydrotalcites (Mantilla, Acatitla, Mendoza, Tzompantzi, & Gomez, 2011), mesoporous TiO_2 film (Rathousky, Kalousek, Kolar, & Jirkovsky, 2011) and Fe(III) citrate complex (Abida, Kolar, Jirkovskyc, & Mailhota, 2012). These materials showed promising photocatalytic efficiency in the degradation of 4-chlorophenol under UV-light irradiation. However, only very few studies have been reported on the degradation of 4-chlorophenol under visible-light illumination. Visible-light assisted photocatalytic degradation of 4-chlorophenol has been carried out using $ZnFe_2O_4$ modified TiO_2 nanotube array electrode (Hou, Li, Zhao, Quan, & Chen, 2010) and mesoporous carbon nitride (Cui, Huang, Fu, & Wang, 2012). Though these materials exhibit good photocatalytic activity, fabrication process using these materials is tedious and not economical. Hence in the present study, we focused to fabricate a simple method using earth abundant source.

Solar energy can be used to degrade hazardous organic chemicals by direct thermal decomposition or by photochemical reaction. Some advantages include savings in fuel use, improved thermal destruction of contaminants, and the reduction of exhaust gas volumes, including products of incomplete combustion (PICs). These processes can use either thermal energy or a range of photochemical reactions. In order to achieve high efficiency to decompose contaminants, the concentration of the radiation is required. This can be achieved by reflecting solar radiation by mirrors (heliostats) and absorbed by a receiver where temperatures of up to 2300 K are reached. High destruction efficiencies can be achieved at temperature much lower than the temperature required for thermal incineration (Shukla, Dorris, & Chikka veeraiah, 2009). An ideal magnetic photocatalyst should possess the following features: (a) high activity in photocatalytic degradation; (b) no photodissolution during degradation; (c) a high magnetization for easy magnetic separation.). The aim of this study is to focus a synthesized Chitosan/$CoFe_2O_4$ nanocomposites (denoted as "CS/CF") initiated by γ-ray irradiation polymerization. The objectives of this study are to investigate the photocatalytic activity of the as synthesized nanocomposite was measured against the 2-chlorophenol (2-CP) under sun light irradiation.

Chitosan (CS) is one of the most important adsorbents with high capacity for the adsorption of organic and inorganic pollutant, which has been widely used in wastewater treatment, (Lulu et al., 2012) because of its high the amino (—NH_2) and hydroxy (—OH) groups of CS chains can coordinate and react with contaminants. Although CS have the potential applications in wastewater treatment, (Chi & Cheng, 2006) it cannot be separated and regenerated from the wastewater. Thus, the addition of magnetic CF nanoparticles make the nanocomposite could be separated from the water by an external magnetic field (Shrestha et al., 2009). Compared with the conventional photocatalytic materials, magnetic/CS nanocomposite not only gave high efficiency in photocatalysis, but also provided excellent magnetic and adsorption properties, which make the nanocomposite easy-recycled and regenerated. Owing to above merits, CS/CF nanocomposites could serve as convenient, effective, and recyclable photocatalysts.

2. Experimental

2.1. Materials

Chitosan (CS) was kindly by pronova Biopolymer, Inc (USA). The degree of deacetylation and molecular weight were determined as 85% and 50,000, respectively. 2-chloro phenol (2-CP) was supplied from Aldrich. Both of them were used as received. Ferric chloride ($FeCl_3{\cdot}6H_2O$, 99.5%), Cobalt chloride ($CoCl_2{\cdot}6H_2O$, 98%) and sodium carbonate anhydrous (Na_2CO_3, 99.5%) were procured from Merck, Darmstadt, Germany. Other chemicals, such as NaOH, were purchased from El-Nasr Co. for chemical industries, Egypt and used without further purification.

2.2. Synthesis of cobalte ferrite $CoFe_2O_4$ (CF)

Cobalte ferrite (CF) were prepared by hydrothermal method (Mishra, Senapati, Borgohain, & Perumal, 2012; Liu, Feng, Xu, Chen, & Wang, 2012). $CoCl_2{\cdot}6H_2O$ (2.381 g in 15 ml of H_2O, 0.01 mol) and $FeCl_3{\cdot}6H_2O$ (5.4058 g in 15 ml of H_2O, 0.02 mol) solutions were mixed and stirred in a magnetic stirrer. Subsequently, 15 ml of NaOH (3.2 g in 15 ml of H_2O, 0.08 mol) and 15 ml of deionized water were added dropwise to the mixed suspension solution and stirred for half an hour at 80 °C. Then, the solution (dark brown) (final total volume = 60 ml) was transferred into an autoclave and kept at 180 °C for 10 h. After this, the resulting black precipitate was washed with water for the complete removal of excess NaOH and other electrolytes. Finally, CF-NP were obtained after sintering at 200 °C for 4 h. The chemical reaction is given as follow:

$$Co^{2+} + 2Fe^{3+} + 8OH^- \rightarrow CoFe_2O_4 + 4H_2O$$

2.3. Preparation of chitosan/$CoFe_2O_4$(CS/CF) nanocomposites

Radiation cross-linking technique was used for the preparation of (CS/CF) nanocomposites. In this specific procedure, a certain amount of CF (0.2 g) nanoparticles was added to the solution with vigorous stirring in order to keep the CF nanoparticles suspended in the solution. 0.1 M of ammonium persulphate which acts as an oxidant was added to 5 ml chitosan solution (0.5 g of CS was dissolved in 30 ml of 1 wt.% acetic acid solution) in a glass tube and the mixture was dispersed with ultrasonic, at room temperature for 20 min. The glass tube was then sealed with Para film and placed in ^{60}Co gamma cell (made in Russia) facility of the National Center for Radiation Research and Technology, Cairo, Egypt. Polymerization was carried out at 10 and 20 kGy at a dose rate of 1.2 kGy/h. The nanocomposite was washed with ethanol and distilled water in turn until pH was about 7. Then, the CS/CF nanocomposite was dried in an oven at 50 °C.

2.4. Characterization

Fourier transform infrared (FTIR) spectra were obtained in the transmission mode using Mattson 1000, Unicam infrared spectrophotometer Cambridge, England. The spectra covered the infrared region 4000 to 400 cm^{-1} using KBr pellets.

Morphological observation was performed using a transmission electron microscope (TEM) JEOL: JEM-100cx). CF powder was dispersed in ethanol using an ultrasonic device, placed on carbon-coated copper grids, and dried under ambient conditions for morphological observation.

Absorbance measurement was carried out on UNICAM UV–vis Spectrometer—1000 Model spectrophotometer.

2.5. Photocatalytic degradation studies and analysis

All experiments were carried out in a batch photoreactor shown in Fig. 1. The photocatalytic reactor was made up of Pyrex glass of 200 ml capacity, and a water circulation arrangement to maintain the temperature at the outer wall of the reactor. The temperature of the reactor was kept constant at 30 °C for all photocatalytic reactions. The reactor assembly was placed on a magnetic stirring plate

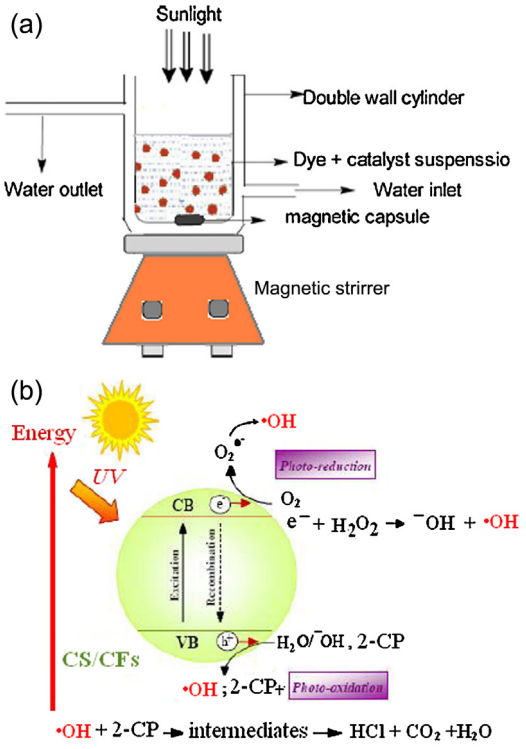

Fig. 1. (a) Schematic diagram of the experimental setup for adsorption and photocatalytic process. (b) Mechanism of photodegradation of 2-CP by CS/CF photocatalyst under sun light.

to further enhance the agitation. Then the whole reaction set-up with reaction mixture was exposed to sunlight with constant stirring for 4 h at a speed of 600 rpm. Photocatalytic experiments were carried out during day time between 11 am and 3 pm in the summer season. In a typical procedure 100 mg of the photocatalyst was added to 100 ml of phenolic solution (100 mg/l) and was sonicated for 15 min. The system was then placed in dark for 30 min to reach the adsorption/desorption equilibrium. After equilibrium, the phenol concentration (nonadsorbed) was detected and taken as initial concentration for photocatalytic process. After that, it was then irradiated with sunlight.

At periodic intervals, about 5 ml was withdrawn and the extent of degradation was then analyzed by spectrophotometer. 2-chloro phenol at alkaline condition reacts with potassium ferricyanide and 4-aminoantipyrine to form a red colored complex. The absorbance of the complex having λ_{max} at 504 nm is a direct measure of phenol concentration (El-Hamshary, El-Sigeny, Abou Taleb, & El-Kelesh, 2007).

The experimental studies were carried out by varying concentrations of phenol within a range of 25–100 ppm. The medium pH was adjusted using 0.1 M HCl or NaOH throughout the experiments.

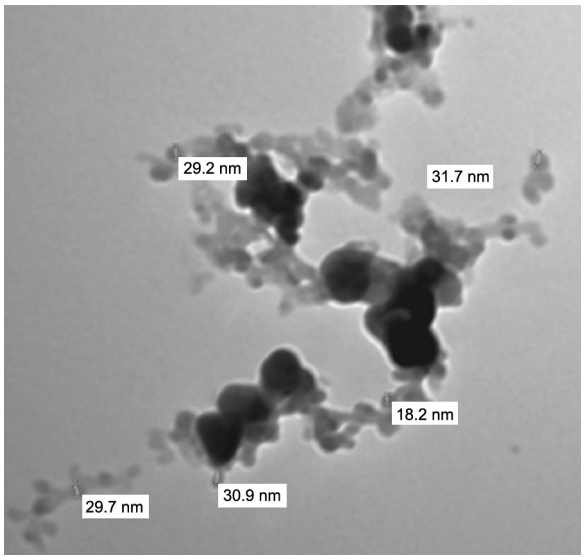

Fig. 2. TEM micrograph of CS/CF nanocomposite with 0.2 wt% of CF-NP.

The suspended catalyst in the aqueous system was oxygenated continuously by the ambient air.

3. Results and discussion

3.1. Polymerization mechanism

CS and CF precursor can coexist in the ionic state when solved in 2% acetic acid aqueous solution. Also, it is known that the surface charge of metal oxide is positive below the pH of the point of zero charge (PZC), while it is negative above PZC. Since the surface of (CF) has PZC of pH ≈ 6, it is positively charged in the acidic conditions (Jiang, Ai, Qin, Liu, & Li, 2009). Since polymerization takes place in acidic medium, therefore, adsorption of an amount of the anions may occur and compensate the positive charges on ferrite surface. Chitosan is converted to cationic ions in acidic conditions as equation below:

$$CS\text{-}NH_2 + CH_3COOH \rightarrow CS\text{-}N^+H_3 + CH3COO^-$$

The free amino group of chitosan (CS-NH_2) was protonated to CS-NH_3 when CS dissolved in acetic acid aqueous solution (Prasanna, Jayanna, Lamani, & Dash, 2011). Thus, the hydrogel composites were formed by the in situ polymerization of the magnetic nanoparticles with monomer solution to physically entrap the magnetic particles in the hydrogel matrix.

The electrostatic interactions occur between anions adsorbed on the CF surface and cationic CS ions. The (CS/CF) are polymerized by gamma radiation copolymerization of the magnetic nanoparticles with CS in acidic aqueous solution to physically entrap the magnetic particles in the matrix as equation below:

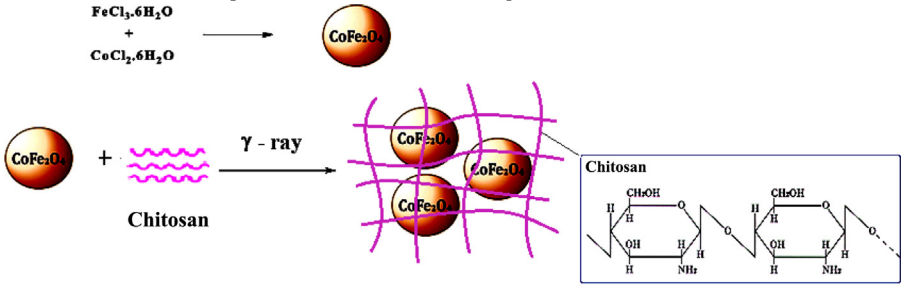

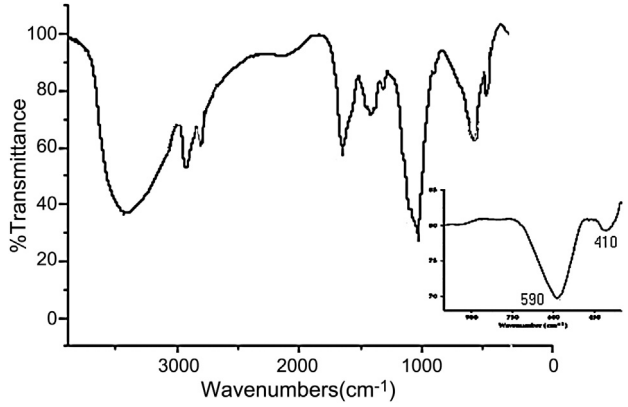

Fig. 3. FTIR spectra of CS/CF nanocomposite with 0.2 wt% of CF-NP.

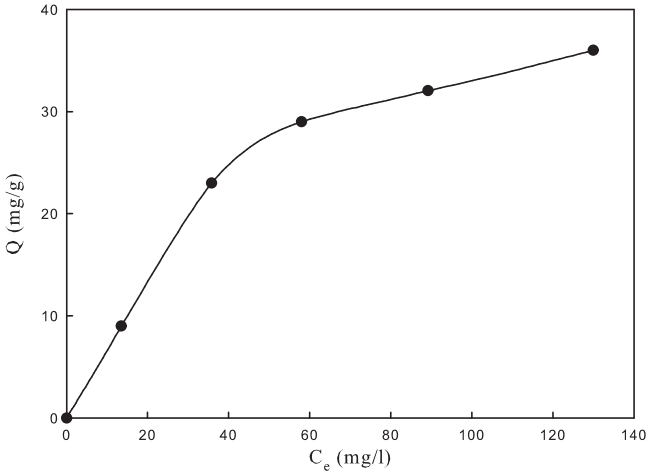

Fig. 4. Adsorption isotherm for 2-CP(mg/g) adsorption onto CS/CF nanocomposite, at 30 °C as a function of equilibrium concentration (C_e) of 2-CP.

3.2. Characterization of (CS/CF) nanoparticles

TEM techniques help to visualize the size and shape of (CS/CF) nanocomposite. Fig. 2 depicts the TEM image of (CS/CF) nanocomposite shown inset cluster. The average diameter of the fine non agglomerated particles was found to be nearly 29 nm, which are highly desirable for the catalytic activity. It is also clear that magnetite particles are completely embedded within chitosan particles due to occurring of two simultaneous processes, one involving formation of magnetite particles and the other involving precipitation of chitosan chains. In addition, the observed agglomerations of nanocomposite particles may probably be due to the absence of stabilization agent in the reaction system as well as due to agglomerating tendency of chitosan (Namdeo & Bajpai, 2008).

3.3. FT-IR characterization

Previous studies have reported that there are two characteristic bands in the infrared spectra of all spinels, particularly ferrites (Mishra et al., 2012; Liu et al., 2012). The highest band υ_1, observed from 600 cm^{-1} to 550 cm^{-1}, corresponds to the intrinsic stretching vibrations of the metal at the tetrahedral site Mtetra ↔ O. The lowest band υ_2, which is observed from 450 cm^{-1} to 385 cm^{-1}, corresponds to the octahedral-metal stretching Mocta ↔ O (Mishra et al., 2012; Liu et al., 2012). According to the classification of Waldron, the vibrations of the unit cell of a cubic spinal can be induced in the A- and B-sites. Hence, the absorption band υ_1 is caused by the stretching vibration of the tetrahedral metal—oxygen bond, whereas the absorption band υ_2 is caused by the metal–oxygen vibration at the octahedral sites.

The FT-IR measurements for the synthesized CS/CF nanocomposite confirm the presence of the aforementioned two characteristic bands (Fig. 3). One is located at 590 cm^{-1}, which corresponds to the tetrahedralmetal stretching vibration. The other is observed at 410 cm^{-1}, which corresponds to the octahedral-metal stretching vibration. The presence of the additional two band at position 590 cm^{-1} and 410 cm^{-1} is the signature band of Fe—O stretching, thus the data revealed that the presence of the CF in CS matrix. These results agree with data from literature (Mishra et al., 2012). The presence of two characteristic absorbance bands centered at 1636 and 1597 cm^{-1}, which correspond to the C—O stretching vibration of —NHCO— (amide I) and the N—H bending of NH_2, respectively in chitosan molecules (Fan et al., 2012).

3.4. Adsorption capacity of 2-CP on the photocatalysts

The adsorption capacities of 2-CP onto CS/CF nanocomposite were performed at different initial concentrations between 25 mg/l and 150 mg/l. The results are shown in Fig. 4. Adsorption isotherm expresses the relationship between the mass of 2-CP adsorbed per unit weight of the CS/CF nanocomposite and equilibrium concentration of 2-CP in solution. The adsorbed quantity is calculated from the following equation:

$$q_e = \frac{(C_0 - C_e)\,V}{W}$$

where q_e is the amount of adsorbate adsorbed per unit mass of adsorbent (mg/g). C_o and C_e are initial concentration (C_o) and the equilibrium concentration (mg/l), respectively, V (l) is the volume of 2-CP solutions and W (g) is the weight of CS/CF nanocomposite. The high adsorption capacity of photocatalysts is a crucial factor required for efficient degradation of pollutant molecules particularly in a low concentration level (Kamat, 1992). The applicability of the isotherm equation to describe the adsorption process was judged by the correlation coefficients, R^2 values. It appears that the isotherm of 2-CP fits the Langmuir adsorption model well.

The Langmuir adsorption isotherm (Fig. 5a), which assumes that the adsorption occurs at specific homogeneous sites within the adsorbent and which has been successfully applied to many monolayer adsorption process (Wang, Boyjoo, & Choueib, 2005), can be written using the following linearized equation (El-Sigeny, Mohamed, & Abou Taleb, 2014):

$$\frac{C_e}{q_e} = \frac{1}{Q_o b} + \frac{1}{Q_o} C_e$$

where q_e (mg/g) is the adsorption capacity at equilibrium, Q_o (mg/g) is the maximum adsorption capacity, C_e (mg/l) is the equilibrium concentration of 2-CP in solution, and b (l/mg) is the effective dissociation constant. The values of R^2, Q_o and b are calculated from the plot in Fig. 5. The values of correlation coefficient, Q_o and b are ($R^2 > 0.98$), 40.272 mg/g and 0.0186 l/g, respectively.

The Freundlich isotherm (Fig. 5b), which describes the adsorption process on energetically heterogeneous surfaces and multilayer sorption, can be written using the following linearized equation (El-Sigeny et al., 2014).

$$\ln q_e = \ln K_f + \frac{1}{n} \ln C_e$$

where K_F and n are Freundlich constants with n giving an indication of how favorable the adsorption process. K_F indicates adsorption capacity (mg/g), and n empirical parameter related to the intensity of adsorption which varies with the heterogeneity of the adsorbent. The slope of $1/n$ ranging between 0 and 1 is a measure of

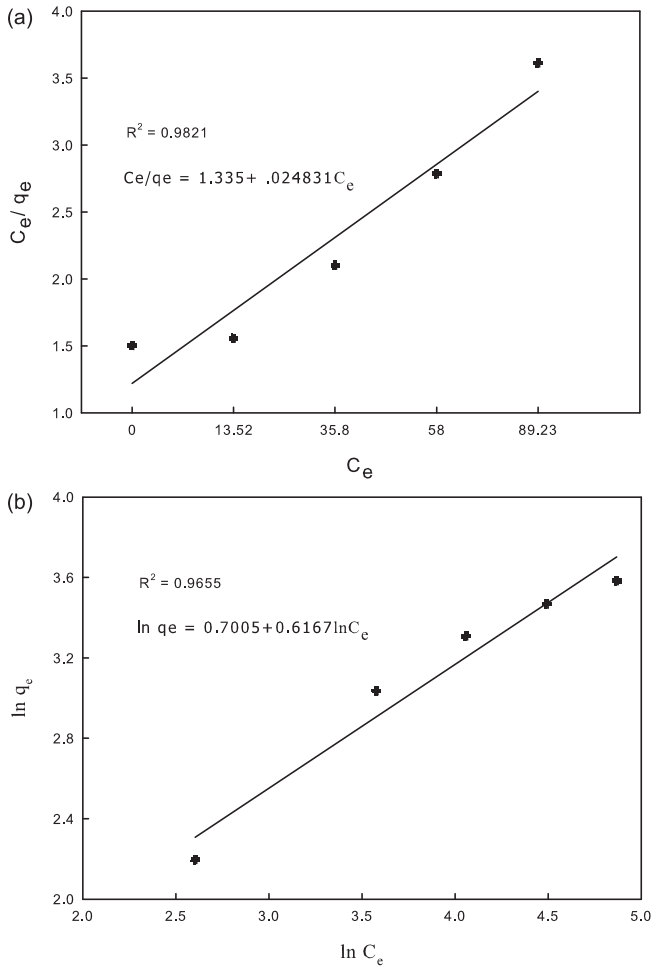

Fig. 5. (a) Langmuir adsorption isotherm for dye adsorption as a function of equilibrium concentration.(b) Linear Freundlish adsorption plots for adsorption of 2-CP onto CS/CF nanocomposite at 30 °C at initial Conc. 100 mg/l.

adsorption intensity or surface heterogeneity, becoming more heterogeneous as its value gets closer to zero (Tan, Ahmad, & Hameed, 2008). A value for $1/n < 1$ indicates a normal Langmuir isotherm while $1/n > 1$ is indicative of cooperative adsorption (difficult to adsorb) (Tan et al., 2008).

The $1/n$ value of 2-CP compound is 0.616 indicating that 2-CP easily adsorbed on the CS/CF nanocomposite.As can be seen, the Langmuir model showed the higher R^2 value (>0.97), suggesting that this model yielded the best fit compared to other models. This indicated that 2-CP adsorbed as a monolayer adsorption process occurs on the homogeneously distributed active sites of CS/CF nanocomposite adsorbent. By using the Langmuir isotherm it is possible to predict whether an adsorption system is favorable or unfavorable through a dimensionless constant referred to as separation factor RL defined by the following equation (El-Sigeny et al., 2014; Chen, Zhao, Wu, & Dai, 2011).

$$R_L = \frac{1}{1 + bC_0}$$

where b (l/mg) is the Langmuir constant and C_0 (mg/l) is the highest initial 2-CP concentration. The value of R_L indicates the type of the isotherm (adsorption process) to be either unfavorable ($R_L > 1$), linear ($R_L = 1$), favorable ($0 < R_L < 1$) or irreversible ($R_L = 0$). R_L values (0.35) related to 2-CP adsorption on CS/CF were less than 1 and greater than 0 indicating a favorable adsorption.

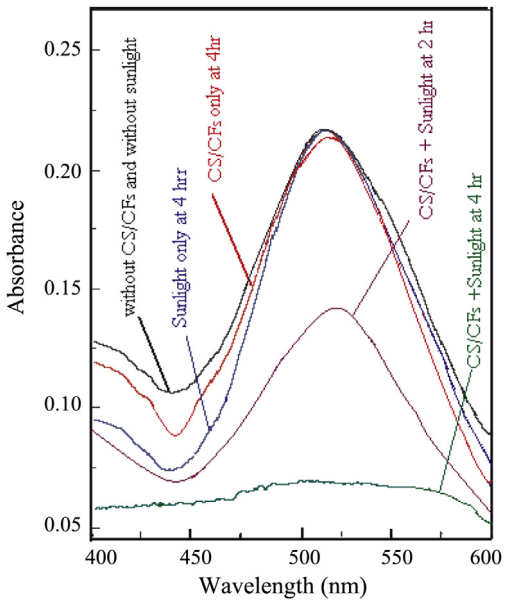

Fig. 6. Absorbance spectra of 2-chlorophenol loaded with and without CS/CF/water and sunlight irradiation for 2 and 4 h.

3.5. Photocatalytic activity

To evaluate the photocatalytic activity of CS/CF nanocomposite, the degradation of 2-CP was investigated at three different experimental conditions: (i) under sunlight in absence of CS/CF (photolysis), (ii) in the dark with CS/CF and (iii) under sunlight in presence of CS/CF (photocatalysis). The absorption spectra, obtained using UV–vis spectrophotometer, are illustrated in Fig. 6. It can be seen that a maximum absorbance was observed around 504 nm for two cases: (i) for the mixture of 2-CP and water in as-mixed state and (ii) when the irradiation was carried out in the absence of CS/CF at 4 h. These results suggest that no 2-CP degradation occurs in these mixtures. In non irradiated suspensions, there was a slight loss, ca. 10%, due to adsorption of 2-CP molecules onto CS/CF (Mishra et al., 2012) (revealed a minor change in the maximum absorption around 504 nm). However, in the presence of CS/CF a rapid degradation of 2-CP occurred by irradiation (maximum absorbance almost disappears). After 2 h irradiation, the peak intensity of 2-CP significantly decreased with an emerging peak which should be ascribed to the most prevalent intermediate (2-CP) (Rao et al., 2003). This result obviously indicates that the presence of CF effectively enhances the photocatalytic activity to degrade 2-CP organic contaminant.

3.6. Effect of 2-chlorophenol (2-CP) concentration

Fig. 7a shows the effect of the initial phenol concentration on the photocatalytic degradation efficiency. The initial phenol concentration in this study was varied from 25 to 100 mg/l. It can be seen from the figure that the degradation efficiency of 2-CP decreased as initial 2-CP concentration increased. Similar results have been presented for the photocatalytic oxidation of other organic compound (Barakat et al., 2004; LengWong, Tan, & Mohamed, 2011). A possible reason is that the generation of hydroxyl radicals on the catalyst surface is reduced when the initial 2-CP concentration is increased. More 2-CP molecules are adsorbed on the surface of CS/CF photocatalyst will make fewer active sites available for the hydroxyl radicals adsorption. Hence, large amounts of adsorbed 2-CP would have an inhibitory influence on the reaction between 2-CP

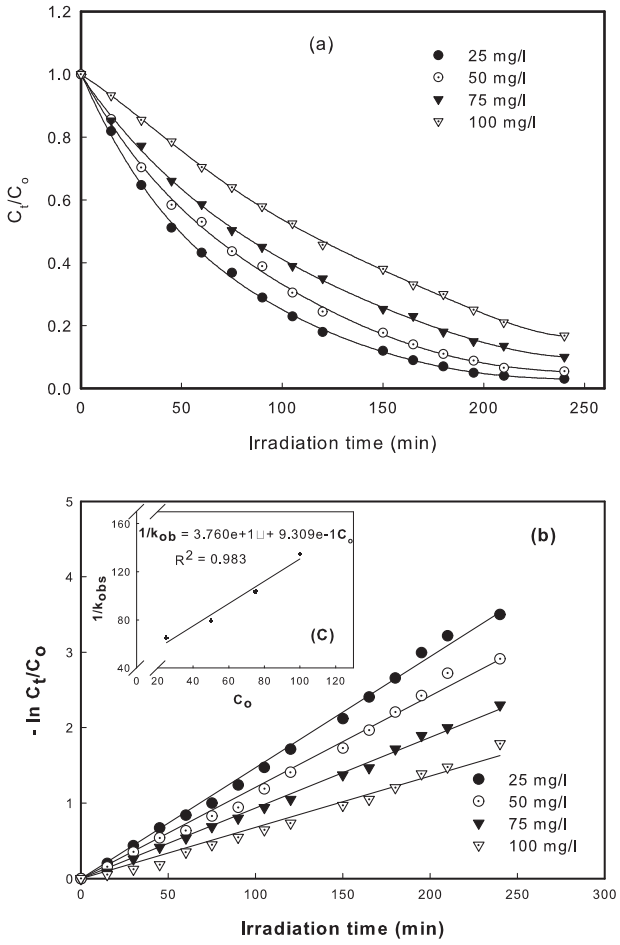

Fig. 7. (a) Effect of irradiation time (min) on photocatalytic degradation of 2-CP onto CS/CF nanocomposite. Control: pH = 6–7; temp.: 30 °C; *t*: 4 h. (b) at different initial concentration (c) first-order photo-degradation kinetics at different initial concentrations.

molecules and hydroxyl radicals due to the lack of any direct contact between them.

Once the 2-CP concentration is increased, most of sun light is absorbed by the 2-CP molecules (Lam, Sin, & Mohamed, 2010), and photons do not reach the surface of photocatalyst to activate it to generate hydroxyl radicals (LengWong et al., 2011).

The photocatalytic degradation follows a pseudo first order reaction and its kinetics can be expressed using relation,

$$\ln\left(\frac{C_0}{C}\right) = k_{obs}t$$

where C_0 is the initial reactant concentration (mg/l) and t the illumination time (min). The apparent rate constant, k_{obs} can be taken as the apparent first order rate constant of the degradation reaction. The linear graph of $-\ln C_0/C$ vs t confirms the first order reaction for the 2-CP degradation at low concentration within the experimental range. The apparent rate constant k_{obs} (min^{-1}) in above equation decreased with the increasing of initial concentration of 2-CP when other parameters are kept unchanged as shown in the insert of Fig. 7b. The appropriate reason for the observed decrease in rate constants when increasing the initial concentration of 2-CP is due to enhanced adsorption of 2-CP at the nanocatalyst surface which thereby prevents the penetration of light into the suspension (Sathishkumar, Pugazhenthiran, Mangalaraja, Asiri, & Anandan, 2013). The derived apparent reaction rate constants (k_{obs}) for the catalysts which have pseudo first-order kinetic and linear regression coefficients are summarized in Table 1. As shown in

Table 1
Pseudo-first order rate constants for the degradation and linear regression coefficients of 2-CP at different initial concentrations and photocatalytic degradation (C_t/C_o) at different pH using CS/CFs as photocatalyst.

C_o (mg/l)	k_{obs} (min^{-1})			R^2
25	0.0153			0.9968
50	0.01256			0.9949
75	0.00966			0.9972
100	0.007414			0.991
Photocatalytic degradation (C_t/C_o) at different pH				
C_o (mg/l)	pH 3	pH 5	pH 7	pH 10
25	0.15	0.1	0.06	0.02

Table 1, the polymeric nanocomposites have higher photocatalytic activity, which is represented by the largest k_{obs} value.

In recent years, the Langmuir–Hinshelwood (L–H) rate expression has been used successfully for heterogeneous photocatalytic degradation to describe the relationship between initial degradation rate and initial concentration (Krishnakumar & Swaminathan, 2011). A linear expression can be conveniently obtained by plotting $1/k_{obs}$ against initial concentration:

$$\frac{1}{k_{obs}} = \frac{1}{k_c K_{LH}} + \frac{C_0}{k_c}$$

where K_{LH} the Langmuir–Hinshelwood adsorption equilibrium constant (l/mg) and k_c the rate constant of surface reaction (mg/l/min). The plot of $1/k_{obs}$ versus C_0 represented in Fig. 7c shows a linear variation, confirming the Langmuir–Hinshelwood relationship for the initial rates of degradation. This indicates that the degradation of 2-CP occurred mainly on the surface of CS/CF nanocomposite. In this study, a reasonable agreement ($R^2 = 0.983$) was obtained between the experimental results and the linear form of the L–H expression. This expression used values of k_c and K_{LH}, calculated from the intercept and the slope of the straight line were 1.074 mg/l/min and 0.155/l/mg, respectively. This indicated that the photodegradation rate of 2-CPcan be described by the Langmuir–Hinshelwood model.

3.7. *Effect of pH*

An important parameter in the photocatalytic reactions taking place on the particulate surfaces is the pH of the solution, since it governs the surface charge properties of the photocatalyst and size of aggregates it forms (Barakat et al., 2004). The effect of pH was studied at different pH values (in the range 3–11) are illustrated in Table 1. The pH of the reaction mixture was adjusted by adding a dilute aqueous solution of HCl or NaOH. Several researches showed that the removal efficiency of 2-CP decreased with increasing pH values.

Degradation efficiency of 2-CP has not been found to be significant at low pH values but increased rapidly with increase of the pH, attaining a maximum value of 95.4% for pH of 10. Further increase in pH showed only a small increase in the photodegradation efficiency. Since the protons are potential determining ions for CF, the surface charge development is affected by the pH (Barakat et al., 2004). Upon hydration, surface hydroxyl groups are formed on CF. A low pH is associated with a positively charged surface which cannot provide hydroxyl groups which are needed for hydroxyl radical formation. Consequently, the rate of 2-CP degradation may decrease. On the other hand, higher pH value can provide higher concentration of hydroxyl ions (OH^-) to react with the holes to form hydroxyl radicals ($OH^{\cdot}$), thereby enhancing the photodegradation of 2-CP (Barakat et al., 2004). The pH decreases during the photodegradation runs and was adjusted by using 0.1 M NaOH. The change in the pH is due to the liberation of HCl during the degradation

reaction. The reaction can be represented mechanistically (Barakat et al., 2004) and stoichiometrically as follows:

$$\underset{(C_6H_4OHCl)}{2\text{-CP}} \xrightarrow{h\nu_1 H_2O} \underset{(C_6H_4(OH)_2}{\text{catechol}} \xrightarrow{h\nu} \text{intermediates} \xrightarrow{h\nu} HCl, CO_2, H_2O$$

$$2C_6H_4OHCl + 13O_2 \rightarrow 2HCl + 12CO_2 + 4H_2O$$

3.8. Photocatalytic reaction mechanism

The proposed mechanism of photocatalytic activity of CS/CF nanocomposite has been introduced in Fig. 1b

In the CS/CF nanocomposite, irradiation with sun light results in the excitation of the surface-adsorbed photosensitizer CS (Eq. (1)), which is acting as an organic semiconductor, followed by the formation of an electron-hole pair on CS. The photogenerated electron transfer into the conducting band of the CF nanocomposite efficiently (Eq. (2)). The electron in the conduction band (e^-_{CB}) is transferred to molecular oxygen, leading to the formation of a series of radicals, which are active oxidizers capable of degrading organic pollutants in the system (Eqs. (3)–(8)). Subsequently, the 2-CP can be degraded through a variety of paths (Eq. (9))(Qiu, Zhang, Mo, & Song, 2008).

$$CS/CF + h_\upsilon \rightarrow CS*/CF \quad (1)$$

$$CS*/CF \rightarrow CS^{\bullet+}/CF + e^-_{CB} \quad (2)$$

$$e^-_{CB} + O_2 \rightarrow {}^\bullet O^-_2 \quad (3)$$

$$H_2O + {}^\bullet O^-_2 \rightarrow {}^\bullet OOH + {}^-OH \quad (4)$$

$$2{}^\bullet OOH \rightarrow O_2 + H_2O_2 \quad (5)$$

$${}^\bullet OOH + H_2O + e^-_{CB} \rightarrow H_2O_2 + {}^-OH \quad (6)$$

$$H_2O_2 + e^-_{CB} \rightarrow {}^\bullet OH_2 + {}^-OH \quad (7)$$

$$H_2O_2 + {}^\bullet O_2{}^- \rightarrow {}^\bullet OH + {}^-OH + O_2 \quad (8)$$

$${}^\bullet OH/{}^\bullet O_2{}^-/CS* + 2\text{-}CO \rightarrow 2HCl + 12CO_2 + 4H_2O \quad (9)$$

3.9. Reusability of photocatalyst

The advantages of the synthesized magnetic nanocomposite are they can be easily separable by the application of external magnetic field after the photocatalytic reaction which avoids the hazardous disposal of photocatalysts to the environment (Sathishkumar et al., 2013). After complete degradation of 2-CP, the catalyst was washed repeatedly with water for several time to remove the adsorbed molecules. The separated catalyst was dried at 200 °C for 2 h and reused. The photocatalytic activity of the recovered CS/CF catalyst was tested thrice under similar conditions. The results revealed that the catalytic activity of the used catalyst did not show any significant loss of activity upto 4 cycles. The observed result illustrates that the photocatalyst was found to be very stable and did not lose its catalytic activity therefore the synthesized nanocatalysts were reusable. It was concluded that after 4 cycle over 80% of 2-CP could be degraded which suggested that the reused CS/CF nanocomposite still remained good activity. The reduced removal efficiency might be caused by two reasons: first, conglomeration of CS/CF nanocomposite led to decrease of activation; second, part of CS/CF nanocomposite might be rinsed during discarding of supernatants (Zhang et al., 2009b).

4. Conclusions

The results of this study show that the CS/CF can efficiently catalyze the decomposition of 2-chlorophenol in the presence of sun light. The reaction rates of photocatalytic degradation of mono-substituted phenols were influenced by pH values, which could affect the surface characteristics of CS/CF and the distribution of reaction species. High photocatalytic efficiency was observed with a medium pH of 10. The photocatalytic degradation of 2-CP performed best at low initial 2-CP concentration as the photocatalytic degradation efficiency decreased with increasing initial phenol concentration. The photocatalytic degradation of 2-CP in aqueous CS/CF suspensions follows a pseudo-first-order kinetics. After four cycles of usage, the photocatalysts suffered only a slight decrease in performance, showing CS/CF nanocomposite have excellent stability and reusability. The observations of these investigations clearly demonstrate the importance of choosing the optimum degradation parameters to obtain high degradation rate, which is essential for any practical application of photocatalytic oxidation processes. These results show that CS/CF nanocomposites could serve as convenient, effective, and recyclable photocatalysts for degradation of 2-CP from wastewater.

Acknowledgement

This study was financially supported by the Deanship of Scientific Research—Salman bin Abdullaziz University under the research project no. 2013/01/164.

References

Abida, O., Kolar, M., Jirkovskyc, J., & Mailhota, G. (2012). Degradation of 4-chlorophenol in aqueous solution photoinduced by Fe(III)–citrate complex. *Photochemical & Photobiological Sciences*, *11*, 794.

Ananpattarachai, J., Kajitvichyanukul, P., & Seraphin, S. (2009). Visible light absorption ability and photocatalytic oxidation activity of various interstitial N-doped TiO_2 prepared from different nitrogen dopants. *Journal of Hazardous Materials*, *168*, 253–261.

Bahnemann, D. (2004). Photocatalytic water treatment: Solar energy applications. *Solar Energy*, *77*, 445–459.

Barakat, M. A., Schaeffer, H., Hayes, G., & Ismat-Shah, S. (2004). Photocatalytic degradation of 2-chlorophenol by co-doped TiO_2 nanoparticles. *Applied Catalysis B: Environmental*, *57*, 23–30.

Casbeer, E., Sharma, V. K., & Li, X.-Z. (2012). Synthesis and photocatalytic activity of ferrites under visible light: A review. *Separation and Purification Technology*, *87*, 1–14.

Chen, H., Zhao, J., Wu, J., & Dai, G. (2011). Isotherm, thermodynamic, kinetics and adsorption mechanism studies of methyl orange by surfactant modified silkworm exuviae. *Journal of Hazardous Materials*, *192*, 246–254.

Chi, F. H., & Cheng, W. P. (2006). Use of chitosan as coagulant to treat wastewater from milk processing plant. *Journal of Polymers and the Environment*, *14*, 411–417.

Cui, Y., Huang, J., Fu, X., & Wang, X. (2012). Metal-free photocatalytic degradation of 4-chlorophenol in water by mesoporous carbon nitride semiconductors. *Catalysis Science & Technology*, *2*, 1396–1402.

El-Hamshary, H., El-Sigeny, S., Abou Taleb, M. F., & El-Kelesh, N. A. (2007). Removal of phenolic compounds using (2-hydroxyethyl methacrylate/acrylamidopyridine) hydrogel prepared by gamma radiation. *Separation and Purification Technology*, *57*(2), 329–337.

El-Sigeny, S., Mohamed, S. K., & Abou Taleb, M. F. (2014). *Radiation synthesis and characterization of styrene/acrylic acid/organophilic montmorillonite hybrid nanocomposite for sorption of dyes from aqueous solutions*, http://dx.doi.org/10.1002/pc.22902 (Article first published online: 4 Feb. 2014)

Fan, L., Luo, C., Li, X., Lu, F., Qiu, H., & Sun, M. (2012). Fabrication of novel magnetic chitosan grafted with graphene oxide to enhance adsorption properties for methyl blue. *Journal of Hazardous Materials*, *215-216*, 272–279.

Gryglik, D., Miller, J. S., & Ledakowicz, S. (2007). Singlet molecular oxygen application for 2-chlorophenol removal. *Journal of Hazardous Materials*, *146*, 502–507.

Hou, Y., Li, X., Zhao, Q., Quan, X., & Chen, G. (2010). Electrochemically assisted photocatalytic degradation of 4-chlorophenol by $ZnFe_2O$+-modified TiO_2 nanotube array electrode under visible light irradiation. *Environmental Science and Technology*, *44*, 5098–5103.

Hu, Y., & Yuan, C. (2005). Low-temperature preparation of photocatalytic TiO_2 thin films from anatase sols. *Journal of Crystal Growth*, *274*, 563–568.

Janda, V., & Svecova, M. (2000). By-products in drinking water disinfection. *Chemicke Listy*, *94*, 905–908.

Jiang, J., Ai, L.-H., Qin, D.-B., Liu, H., & Li, L.-C. (2009). Preparation and characterization of electromagnetic functionalized polyaniline/$BaFe_{12}O_{19}$ composites. *Synthetic Metals*, *159*(7–8), 695–699.

Kamat, K. V. P. V. (1992). Photochemistry on surfaces: Photodegradation of 1,3-diphenylisobenzofuran over metal oxide particles. *Journal of Physical Chemistry*, *96*, 5053–5059.

Krishnakumar, B., & Swaminathan, M. (2011). Influence of operational parameters on photocatalytic degradation of a genotoxic azo dye acid violet 7 in aqueous ZnO

suspensions. *Spectrochimica Acta A: Molecular and Biomolecular Spectroscopy*, *81*, 739–744.

Ku, Y., Li, Y. C., Wang, W. Y., Ma, C. M., & Chou, Y. C. (2010). Effect of platinum on the photocatalytic decomposition of 2-chlorophenol in aqueous solution by UV/TiO_2. *Journal of the Chinese Institute Engineers*, *33*, 591–596.

Lam, S. M., Sin, J. C., & Mohamed, A. R. (2010). Parameter effect on photocatalytic degradation of phenol using TiO_2-P25/activated carbon (AC). *Korean Journal of Chemical Engineering*, *27*(4), 1109–1116.

LengWong, C., Tan, Y. N., & Mohamed, A. (2011). Photocatalytic degradation of phenol using immobilized TiO_2 nanotube photocatalysts. *Journal of Nanotechnology*, http://dx.doi.org/10.1155/2011/904629. Article ID 904629, 9 pages

Liu, Shou-Qing, Feng, Lian-Rong, Xu, N., Chen, Zhi-Gang, & Wang, Xiao-Mei. (2012). Magnetic nickel ferrite as a heterogeneous photo-Fenton catalyst for the degradation of rhodamine B in the presence of oxalic acid. *Chemical Engineering Journal*, *203*, 432–439.

Lulu, F., Chuannan, L., Xiangjun, L., Fuguang, L., Huamin, Q., & Min, S. (2012). Fabrication of novel magnetic chitosan grafted with graphene oxide to enhance adsorption properties for methyl blue. *Journal of Hazardous Materials*, *215–216*(2012), 272–279.

Mantilla, A., Acatitla, G. J., Mendoza, G. M., Tzompantzi, F., & Gomez, R. (2011). Photoassisted degradation of 4-chlorophenol and *p*-cresol using MgAl hydrotalcites. *Industrial and Engineering Chemistry Research*, *50*, 2762–2767.

Mishra, D., Senapati, K. K., Borgohain, C., & Perumal, A. (2012). $CoFe_2O_4$–Fe_3O_4 magnetic nanocomposites as photocatalyst for the degradation of methyl orange dye. *Journal of Nanotechnology*, *2012*, 1–6. Article ID 323145.

Mogyor´si, K., Farkas, A., Dékny, I., Ilisz, I., & Dombi, A. (2002). TiO_2-based photocatalytic degradation of 2-chlorophenol adsorbed on hydrophobic clay. *Environmental Science and Technology*, *36*, 3618–3624.

Namdeo, M., & Bajpai, S. K. (2008). Chitosan–magnetite nanocomposites (CMNs) as magnetic carrier particles for removal of Fe(III) from aqueous solutions. *Colloids and Surfaces A: Physicochemical and Engineering Aspects*, *320*, 161–168.

Palanisamy, B., Babu, C. M., Sundaravel, B., Anandan, S., & Murugesan, V. (2013). Sol–gel synthesis of mesoporous mixed Fe_2O_3/TiO_2 photocatalyst: Application for degradation of 4-chlorophenol. *Journal of Hazardous Materials*, *252-253*, 233–242.

Prasanna, G. D., Jayanna, H. S., Lamani, A. R., & Dash, S. (2011). Polyaniline/$CoFe_2O_4$ nanocomposites: A novel synthesis, characterization and magnetic properties. *Synthetic Metals*, *161*, 2306–2311.

Qiu, R., Zhang, D., Mo, Y., & Song, L. (2008). Photocatalytic activity of polymer-modified ZnO under visible light irradiation. *Journal of Hazardous Materials*, *156*, 80–85.

Qourza, S., Barka, N., Tamimi, M., Assabbane, A., & Ait-Ichou, Y. (2008). Photodegradation of 2-naphthol in water by artificial light illumination using TiO_2 photocatalyst: Identification of intermediates and the reaction pathway. *Applied Catalysis A: General*, *334*, 386–393.

Rao, N. N., Dubey, A. K., Mohanty, S., Khare, P., Jain, R., & Kaul, S. N. (2003). Photocatalytic degradation of 2-chlorophenol: A study of kinetics, intermediates and biodegradability. *Journal of Hazardous Materials*, *B101*, 301–314.

Rathousky, J., Kalousek, V., Kolar, M., & Jirkovsky, J. (2011). Mesoporous films of TiO_2 as efficient photocatalysts for the purification of water. *Photochemistry & Photobiological Sciences*, *10*, 419–424.

Sathishkumar, P., Pugazhenthiran, N., Mangalaraja, R. V., Asiri, A. M., & Anandan, S. (2013). ZnO supported $CoFe_2O_4$ nanophotocatalysts for the mineralization of Direct Blue 71 in aqueous environments. *Journal of Hazardous Materials*, *B101*, 171–179, 252-253.

Shafi, K. V. P. M., Gedanken, A., Prozorov, R., & Balogh, J. (1998). Sonochemical preparation and size-dependent properties of nanostructured $CoFe_2O_4$ particles. *Chemistry of Materials*, *10*(11), 3445–3450.

Shrestha, N., Macak, J., Schmidt-Stein, F., Hahn, R., Mierke, C., Fabry, B., & Schmuki, P. (2009). Magnetically guided titania nanotubes for site-selective photocatalysis and drug release. *Angewandte Chemie International Edition*, *48*, 969–972.

Shukla, S. S., Dorris, K. L., & Chikka veeraiah, B. V. (2009). Photocatalytic degradation of 2,4-dinitrophenol. *Journal of Hazardous Materials*, *164*, 310–314.

Sivalingam, G., & Madras, G. (2004). Photocatalytic degradation of poly (bisphenol-A-carbonate) in solution over combustion-synthesized TiO_2: Mechanism and kinetics. *Applied Catalysis A: General*, *269*, 81–90.

Sobczyński, A., Duczmal, Ł., & Zmudziński, W. (2004). Phenol destruction by photocatalysis on TiO_2: An attempt to solve the reaction mechanism. *Journal of Molecular Catalysis A: Chemical*, *213*, 225–230.

Song, S. H., & Kang, M. (2008). Decomposition of 2-chlorophenol using a tourmaline—Photocatalytic system. *Journal of Industrial and Engineering Chemistry*, *14*, 785–791.

Tan, I. A. W., Ahmad, A. L., & Hameed, B. H. (2008). Adsorption of basic dye on high-surface-area activated carbon prepared from coconut husk: Equilibrium, kinetic and thermodynamic studies. *Journal of Hazardous Materials*, *154*, 337–346.

Wang, S., Boyjoo, Y., & Choueib, A. (2005). A comparative study of dye removal using fly ash treated by different methods. *Chemosphere*, *60*, 1401–1407.

Yue, B., Zhou, Y., Xu, J. Y., Wu, Z. Z., Zhang, X., Zou, Y. F., & Jin, S. L. (2002). Photocatalytic degradation of aqueous 4-chlorophenol by silica-immobilized polyoxometalates. *Environmental Science and Technology*, *36*, 1325–1329.

Zhang, H., Chen, G., & Bahnemann, D. W. (2009). Photoelectrocatalytic materials for environmental applications. *Journal of Materials Chemistry*, *19*(29), 5089–5121.

Zhang, S., Zhao, X., Niu, H., Shi, Y., Cai, Y., & Jiang, G. (2009). Superparamagnetic Fe_3O_4 nanoparticles as catalysts for the catalytic oxidation of phenolic and aniline compounds. *Journal of Hazardous Materials*, *167*, 560–566.

Zhu, Y., Stubbs, L. P., Ho, F., et al. (2010). Magnetic nanocomposites: A new perspective in catalysis. *ChemCatChem*, *2*(4), 365–374.

Zi, Z., Sun, Y., Zhu, X., Yang, Z., Dai, J., & Song, W. (2009). Synthesis and magnetic properties of $CoFe_2O_4$ ferrite nanoparticles. *Journal of Magnetism and Magnetic Materials*, *321*, 1251–1255.